DE90005226

NUMERICAL SIMULATION OF LIQUID CIRCULATION IN A BUBBLY COLUMN

WEST VIRGINIA UNIV., MORGANTOWN. DEPT.
OF MECHANICAL AND AEROSPACE ENGINEERING

1990

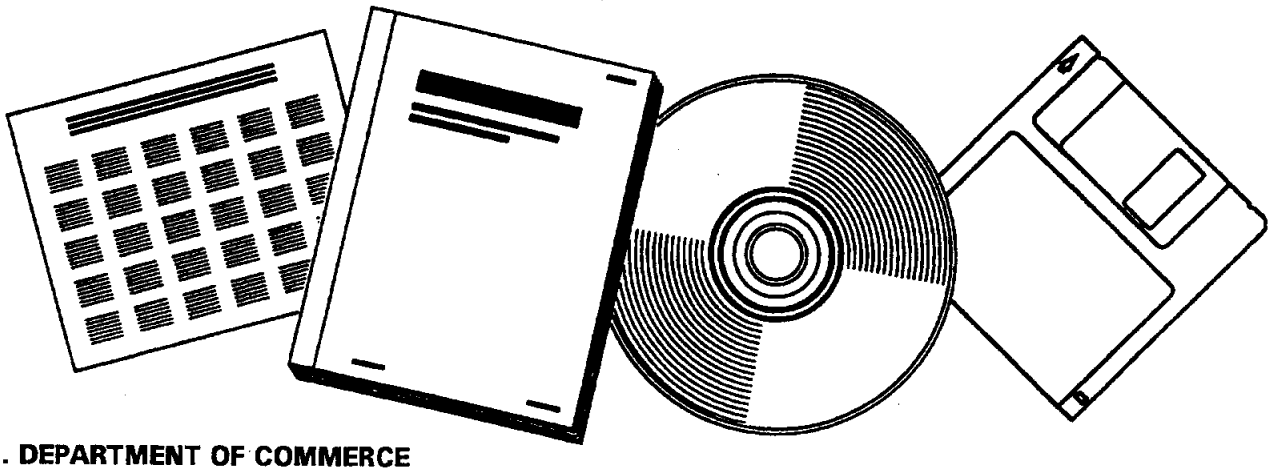

U.S. DEPARTMENT OF COMMERCE
National Technical Information Service

CONF-9006107--1

NUMERICAL SIMULATION OF LIQUID CIRCULATION IN A BUBBLY COLUMN

Ismail Celik and Yi-Zun Wang

Department of Mechanical and Aerospace Engineering
West Virginia University
Morgantown, WV 26506-6101

DOE/PC/79935--13
DE90 005226

ABSTRACT

The gas-liquid flow inside a vertically situated circular, isothermal column reactor has been simulated numerically. The gas-liquid flow is assumed to be in the bubbly flow regime which is characterized by a suspension of discrete air bubbles in a continuous liquid phase such as glycerol water. The mathematical formulation is based on the conservation of mass and momentum principle for the liquid phase. The gas velocity distribution is calculated via an empirically prescribed slip velocity as a function of void fraction. The interface viscous drag forces are prescribed empirically. A profile shape is assumed for the void ratio distribution and the magnitude of it is calculated as part of the solution. The influence of various profile shapes is investigated. Results with the void ratio distribution calculated from the conservation of mass equation for the gas phase are also presented. The mathematical model has been implemented by modifying a readily available computer code for single phase newtonian fluid flows. The numerical discretization is based on a finite volume approach.

The numerical predictions show a reasonably good agreement with measurements. The circulation pattern seems not to be so sensitive to the actual shape of the void fraction profiles, but the inlet distribution of it is important.

Submitted for presentation at the Symposium on "Numerical Methods for Multiphase Flows", ASME/FED Spring Conference, Toronto, Ontario, Canada, June 3-9, 1990.

DISCLAIMER

1. INTRODUCTION

The study of the circulation patterns inside a column reactor is of theoretical and practical significance. because of their wide use in the industry as chemical or bio-chemical reactors. The bubble column reactors offer several advantages over conventional fixed bed reactors: e.g. lower hydrogen to monoxide ratios can be tolerated and hot-spots are controlled in the bed so that catalyst deactivation is reduced. The gas may be introduced evenly through a distributor plate into the slurry, so the circulation patterns of continuous liquid phase can be controlled (Clark, et al, 1990).

Experimental investigation of such reactors have been reported in the literature by many researchers for a variety of flow situations (Rietema and Ottengraf, 1970; Hills, 1974; Rietema, 1982; Freedman and Davidson, 1969; Lamont, 1958; Steinemann and Buchholz, 1984), but comprehensive numerical simulations of the such systems is given little attention. This is not surprising in view of the fact that the mathematical formulation for multi-phase flows is in a stage of development. There is no definite form of the governing equations which is generally accepted (for a review, see Stewart and Wendroff, 1984). Other difficulties such as handling of interaction terms (interface conditions). the boundary and initial conditions and interphase instabilities, make comprehensive numerical modeling a challeging research area and it cails for more attention from the computational fluid dynamisists.

This paper reports on the results of a study where the flow and the circulation patterns inside an isothermal column reactor model, in bubbly flow regime, has been simulated numerically. As a first step, only the equation of motion and continuity for the continuous phase have been solved using a finite volume technique. The gas velocity field is prescribed empirically. Only

the bubbly flow regime is considered. This is done to avoid the complexities of a turbulence closure model at higher superficial gas velocities. These results constitute the first stage of an ongoing research where the numerical solution of the continuum equations of motion for both phases are aimed at where the only empiricism comes through the prescription of interfacial momentum exchange terms.

2. MATHEMATICAL MODEL

The mathematical model is based upon the conservation of mass and momentum for the liquid and gas phases including appropriate interface momentum exchange terms. Invoking continuum assumptions and performing a space or time averaging over a macroscopic control volume. (see e.g., Anderson and Jackson. 1967; Homsy, 1983; Drew, 1983), these equations can be written in cylinderical coordinates (for more details, see Clark et al., 1990) as:

Continuity

$$\frac{\partial}{\partial x}(\rho_1 u_1) + \frac{1}{r}\frac{\partial}{\partial r}(\rho_1 r v_1) = 0 \qquad (1)$$

x - Momentum

$$\frac{\partial}{\partial x}(\rho_1 u_1 u_1) + \frac{1}{r}\frac{\partial}{\partial r}(r\rho_1 u_1 v_1) = -(1-\alpha)\frac{\partial P}{\partial x} - \rho_1 g + F_{12}(u_2-u_1)$$

$$+ \frac{\partial}{\partial x}(\mu_\ell \frac{\partial u_1}{\partial x}) + \frac{1}{r}\frac{\partial}{\partial r}(r\mu_\ell \frac{\partial u_1}{\partial r}) + \frac{\partial}{\partial x}(\mu_\ell \frac{\partial u_1}{\partial x}) + \frac{1}{r}\frac{\partial}{\partial r}(r\mu_\ell \frac{\partial v_1}{\partial x}) \qquad (2)$$

r - Momentum

$$\frac{\partial}{\partial x}(\rho_1 u_1 v_1) + \frac{1}{r}\frac{\partial}{\partial r}(r\rho_1 v_1 v_1) = -(1-\alpha)\frac{\partial P}{\partial r} + F_{12}(v_2-v_1)$$

$$+ \frac{\partial}{\partial x}(\mu_\ell \frac{\partial v_1}{\partial x}) + \frac{1}{r}\frac{\partial}{\partial r}(r\mu_\ell \frac{\partial v_1}{\partial r}) + \frac{1}{r}\frac{\partial}{\partial r}(r\mu_\ell \frac{\partial v_1}{\partial r}) + \frac{\partial}{\partial x}(\mu_\ell \frac{\partial u_1}{\partial r}) - \mu_\ell \frac{2v_1}{r^2} \qquad (3)$$

where the subcripts "1" and "2" or "ℓ" and "g" denote phase-1 (liquid) and phase-2 (gas) respectively; α is the void fraction (i.e. volume concentration of gas), $\rho_1=(1-\alpha)\rho_\ell$, $\rho_2=\alpha\rho_g$ are the macroscopic densities, ρ_ℓ and ρ_g being the microscopic liquid and gas densities, respectively; u and v are the liquid and gas velocities in the x- and r- directions, respectively; g is the acceleration of gravity, μ is the viscosity, P is the pressure, and F_{12} is the momentum exchange function between phase-1 and phase-2.

The equations for the gas phase can be obtained from Eqs. (1) to (3) by changing the subscripts "1" to "2", as well as "ℓ" and "g".

The global assumptions involved in deriving Eqs. (1) to (3) are: isothermal steady, axisymmetric, incompressible flow without swirl and without chemical reactions.

Further it should be noted that the way the pressure gradient terms should be handled in Eqs. (1) - (3) is a controversial issue. There is considerable debate in the literature (see for example Stewart et al., 1984) whether $\nabla[(1-\alpha)P]$ or $(1-\alpha)\nabla P$ should be used in these equations. Both forms satisfy the condition that when the corresponding momentum equations for the two phases are added, the resulting pressure gradient term must be ∇P. The equal pressure model (Stewart et al., 1984) is adopted, i.e. $P_1=P_2=P$; this pressure is distributed as $(1-\alpha)P$ and αP between the liquid and gas phases, respectively. In this regard, the pressure gradient terms are being treated as part of the interfacial momentum exchange. The surface tension effects are neglected in the present study.

If F_{12} is prescribed empirically (see next section), Eqs.(1) through (3) written for both phases constitute a closed set of 6 differential equations for the 6 unknowns, namely α, P, u_1, v_1, u_2 and v_2. As a first step, these

equations are reduced to 4 equations and 4 unknowns by assuming a slip velocity relation of the form

$$\underline{u}_S = \underline{u}_2 - \underline{u}_1 = f(\alpha, Re_b) \tag{4}$$

This explicit form of Eq.(4) is discussed later in the text.

Interfacial Momentum Exchange

The momentum transfer between the different phases takes place via several mechanisms, the most important of which being the viscous drag force resulting from the shear stress at the interface and the form drag due to the pressure distribution on the surface of individual bubbles. Other possible mechanisms for momentum transfer include added mass effect, magnus effect (due to rotation), pressure gradient, and shear rate effects of the surrounding fluid (see for example Hinze, 1972). For brevity these forces will not be considered in the present analysis. Instead, all these effects will be lumped into the function F_{12}.

In the bubbly flow regime, the total drag force can be related to that of a single bubble. Hirt (1982) used the following relation for water droplets in steam (for our problem, ρ_g is replaced by ρ_ℓ).

$$F_{12} = \frac{3}{4}\alpha^2(1-\alpha)\,\rho_g\,\frac{|\underline{u}_1 - \underline{u}_2|}{d_p}\,C_D \tag{5}$$

Where d_p is the droplet diameter and C_D is the drag coefficient for an isolated droplet.

As a first approximation Eq.(5) is used for the bubbly flow regime of this study where C_D is replaced by an empirical relation for bubbles in water.

Such a C_D relation can be derived by curve fitting to the experimental data presented by Clift et al. (1978). For bubbles in pure systems, the following function is suggested by us,

$$C_D = a\, Re_b^{-b} \tag{6}$$

where Re_b is the bubble Reynolds number defined as

$$Re_b = \frac{\rho_\ell |u_2 - u_1| d_b}{\mu_\ell}$$

The coefficients a and b are given in Table 1 for different Reynolds number ranges. This particular form is adapted because it simplifies the calculation of slip velocities considerably.

Table 1. Coefficients for Eq.(6) for Air Bubbles in Pure Liquids

Re_b range	a	b
0 - 2	24	1.000
2 - 10	23.66	0.981
10 - 100	14.9	0.780
100 - 1000	6.9	0.613

Simplification for the Gas Phase

Instead of solving for the gas momentum equations, the gas velocities are determined from a slip velocity relation of the form of Eq.(4). For small void ratios (i.e. dilute flow with a dispersed gas phase) the gas velocities can be calculated in the radial and axial-direction, respectively, as

$$v_s = 0 \quad \text{or} \quad v_\ell = v_g \tag{7}$$

$$u_g = u_s + u_\ell \tag{8}$$

where the slip velocity

$$u_s = U_{b\infty}(1-\alpha) \tag{9}$$

$U_{b\infty}$ is the terminal velocity of an isolated bubble in an infinite liquid medium. The effect of void ratio, α, on the slip velocity as given in Eq.(8) is suggested by Wallis (1962). $U_{b\infty}$ can be calculated by equating the drag force to the difference of the buoyancy force and the weight of the bubble. With the drag

relation. Eq.6, this force balance results in

$$U_{b\infty} = \left[\frac{4}{3a} \frac{(\rho_\ell - \rho_g)}{\rho_\ell} g\, d_b \left(\frac{\rho_\ell d_b}{\mu_\ell} \right)^b \right]^{1/(2-b)} \qquad (10)$$

For example with b = 1 and a = 24. (i.e., Stokes range) Eq.10 reduces to

$$U_{b\infty} = \frac{1}{18} \frac{(\rho_\ell - \rho_g)}{\mu_\ell} g\, d_b^2 \qquad (11)$$

If the water (or liquid) is not pure, the degree of contamination may have significant influence on $U_{b\infty}$. For such cases, the empirical data presented by Clift et al. (1978) can be used. Another alternative is to use the terminal velocity relations presented by Hewitt (1982, chapter 2) where the terminal velocity of bubbles in clean fluids is expressed as a function of Re_b and the Galileo number $G_a = g\mu_\ell/\rho_\ell\sigma^3$.

Profiles for α - distribution

As a further simplification in the present model, $\alpha(x,r)$ is assumed to vary only in the r-direction, and the shape of the profiles $\alpha=\alpha(r)$ are prescribed empirically. Among various shapes investigated are linear, parabolic and consine profiles. The consine profile, for example is given by

$$\alpha(r) = \begin{cases} 0.5\, \alpha_c \left[1+\cos(\pi r/r_s)\right] & r \le r_s \\ 0 & r_s < r \le R \end{cases} \qquad (12)$$

where R is the column radius and r_s is the radius of the bubble street as observed from experiments (Rietema and Ottengraf, 1970). Eq.12 represents a smooth function which satisfies the zero derevative conditions at r=0 and $r=r_s$. The center line value α_c is determined from

$$Q_a = 2\pi \int_0^R \alpha(r) u_g(x,r) r dr \qquad (13)$$

to ensure continuity for the gas phase. Calculations are also performed where $\alpha(x,r)$ is calculated from conservation of mass equation for the gas phase:

$$\frac{\partial}{\partial x} (\alpha u_2) + \frac{1}{r} \frac{\partial}{\partial r} (r \alpha u_2) = 0 \qquad (14)$$

The advantage of prescribing the α-profiles instead of determining from Eg.(14) is to eliminate all the computational uncertainties in solving Eq.(14), such as numerical diffusion. Further, the former makes it possible to investigate the influence of various α-profiles on the circulation patterns.

3. NUMERICAL METHOD

The form of equations for the continuous liquid phase (Eqs.2 and 3) is amenable for using the finite volume technique (e.g. Patankar, 1980) which has been successfully used for solution of steady, incompressible, single phase, recirculating flow problems. This formulation takes into account density variation (say due to buoyancy effects) in space which is suitable for the present problem where the microscopic density is constant but the macroscrpic density varies according to $\rho_1=\rho_\ell(1-\alpha)$. The so called "SIMPLE" algorithm of Patankar (1980) is employed to calculate the pressure field iteratively. However, modification have been made to account for the modified pressure gradients $(1-\alpha)\partial P/\partial x$ and $(1-\alpha)\partial P/\partial r$, and additional momentum source terms $F_{12}(u_2-u_1)$ and $F_{12}(v_2-v_1)$. These modifications have been incorporated in a readily available computer code, TEACH (Gosman and Ideriah, 1976; Durst and Loy, 1984) and the modified version has been used for the present calculations.

The "hybrid" difference scheme is used in the formulation. This scheme

has the property that it switches from centeral to upwind differencing for high Pecklet numbers ($Pe=\rho_1 \Delta x u_\ell/\mu_\ell$) for the convective terms; for the diffusive terms, the central differencing is employed at all times. For the present application the maximum Pe had an order of magnitude of 1.0. That is, the flow was mainly dominated by viscous forces. and the central differencing is used for most of the flow region. This is an important feature of the method especially for calculating the void fraction distribution from Eq.(14) which has no physical diffusion. Since the central differencing is a second order accurate scheme, it minimizes the numerical diffusion.

Boundary Conditions

No slip condition was enforced for the liquid velocities at the walls and at the air inlet (distributor plate); at the centerline (r=0) symmetry conditions were imposed. The free surface was assumed to be undisturbed at which the axial-velocity, u_ℓ, was set equal zero (i.e. no liquid flux through the surface). The radial velocity, v_ℓ, at the free surface was calculated from the condition $\partial v_\ell/\partial x=0$; this is a somewhat arbitrary condition used as a first approximation since no other information is available on v_ℓ.

Boundary conditions are needed for α when it is calculated from Eq.(14). Since there is no mass flux through the walls $\partial\alpha/\partial r=0$ was used at the side walls; the same condition applies at the centerline due to symmetry. At the inlet, a uniform distribution $\alpha=\alpha_o$ was assumed, and α_o was estimated from the number of holes on the distributor plate, i.e., $\alpha_o=\Sigma A_j/A$, $j=1,2,....N$, A_j is the area of an individual hole, A is the total cross-sectional area of the inlet, and N is the number of the holes. Then from Eq.(13) the gas velocity is calculation for a given air flow rate, Q_a.

The α values at the free surface are not needed for the calculations. $\alpha=1$ was imposed at the grid points just outside the free surface. The present

method uses a staggered grid arrangement in which the velocities are staggered and the scalar quantities are stored at centers of main grid cells. The gas velocity at the free surface is calculated from Eq.(13) to satisfy continuity once α was determined there. (see Clark et al., 1990, for particular details)

Convergence and Grid Independence

To ensure properly converged numerical solutions, not only the total residues of difference equations are checked, but also the net liquid circulation, Q_{net} and the maximum relative change in the axial velocity, $\Delta u_{max}/u_{max}$. The net liquid volume circulated shouid be zero for the present problem. This is normalized by the recirculated liquid volume, Q_{cir}, given by

$$Q_{cir} = 2\pi \int_0^{r_o} (1-\alpha)\, u_\ell\, r\, dr = -2\pi \int_{r_o}^{R} (1-\alpha)\, u_\ell\, r\, dr \qquad (15)$$

where r_o is the zero cross point for u_ℓ. After about 300 iterations, both Q_{net}/Q_{cir} and $\Delta u_{max}/u_{max}$ values were less than 10^{-5}. Calculations were continued another 200 iterations to ensure complete convergence.

Two uniform grid distributions were used, namely a coarse grid of 21x12 (Δx=4cm, Δr=1cm), and a fine grid of 42x23 (Δx=2cm and Δr=0.5cm). The difference in liquid velocity from the coarse grid and fine grid solutions was less than 1%. The fine grid solutions are presented in this paper unless stated otherwise.

4. DESCRIPTION OF CASES STUDIED

The numerical study simulated as closely as possible, the experiments performed by Rietema and Ottengraf (1970) where a laminar liquid circulation and bubble street formation were investigated in a Quickfit glass column. The geometric configuration for the glass column is shown in Fig.1. The

experimental conditions for the numerically simulated case were: liquid (glycerol water solution) density ρ_ℓ =1153 kg/m^3, liquid viscosity μ_ℓ=0.35kg/m-s, air flow rate Q_a=11.4cm^3/s, gas hold-up ε_g=74 cm^3, bubble diameter d_b=0.54 cm and bubble street diameter D_S=10.0 cm. The glass column had a diameter of 22 cm and a height of 122cm. Initially the column was filled with the liquid solution up to a depth of 80 cm. If the gas hold-up of 74 cm^3 is added to the liquid volume, the total mixture volume requires a column height of approximately 82 cm. This value was used in the simulations. Air bubbles were formed by means of injection needles. According to experiments, vertical baffles were placed along the wall, so that a reasonably symmetrical street could be created. The effect of the baffles is not considered in the present study.

For the set of calculations where $\alpha(x,r)$ is obtained from the solution of Eq.(14), a step function $\alpha=\alpha_o$ for $r \leq r_s$; $\alpha_o=0$ for $r > r_s$ was assumed (see Fig.3b. α_o was approximated as the area fraction of injection holes to the total area. A hole diameter of 0.5 d_b was assumed. r_s/R values were varied between 0.3 and 0.9 to study the influence of distribution at the inlet on the overall circulation patterns.

4. RESULT AND DISCUSSION

Results with Prescribed α - Profiles

The results of the calculations using a cosine profile for the shape of $\alpha(r)$ distribution are depicted in Fig.2. The predicted streamlines plotted in Fig.2a show the commonly observed circulation pattern with a downward flow near the wall and an upward flow near the center of the reactor. The stream function is calculated from

$$\Psi = 2\pi \int_0^R (1-\alpha)\, \rho_\ell\, u_\ell\, r\, dr \qquad (16)$$

The total volume of liquid circulation can be read off from Fig.2a as $Q_{cir} \cong 0.16 m^3/s$. The center of the circulation zone is predicted to be very close to the free surface. As it will be discussed later, the circulation pattern is a direct result of the void-fraction distribution. The corresponding α distribution is shown in Fig.2b; Though the shape of the α-distribution is assumed, its magnitude is calculated as part of the solution. Fig.2b shows that α decreases with the axial distance. This occurs as a result of the increase in the gas velocity towards the free surface; to satisfy continuity (Eq.13) as the mean value of u_g increases, that of α should decrease. The predicted liquid velocity profiles are shown in Fig.2c. The predicted value of centerline velocity, $u_{\ell C}$=22 cm/s, at x/L=0.5 is considerably higher than the measured value of $u_{\ell C}$=10.5 cm (see also Fig.2c). The boundary of the reverse flow where u_ℓ=0 is predicted as r_O=0.50 which is in good agreement with experiments. The agreement is also good for the maximum reverse flow velocities which are seen to be 3-4 and 3-5 cm/s for experiments and predictions, respectively. Of course, these quantities do change with axial distance and with the prescribed bubble-street radius, r_S.

Calculations performed with various street radii show that a decrease in r_S causes an increase in α values, thus an increase in the liquid velocity and vise versa. This also affects the boundary of the reverse flow zone. For example, for r_S/R=0.65, the predicted centerline velocity was about 18cm/s and r_O/R=0.52 at the mid-hight of the column. Consequantly, the uncertainties in measuring the region where $\alpha \cong 0$ (i.e. no air bubbles) will result in differences between the experiments and predictions.

The influence of different void fraction-profile shapes on the results were

also investigated where the gas flow rate and the bubble-street diameter were fixed. The linear and parabolic α-profiles did not influence the results very much. The reverse flow boundary and the maximum reverse flow velocities were affected the least. The centerline liquid velocity was somewhat higher for the parabolic profile compared to the others. These results show that it is the magnitute of the α-distribution and the bubble-street diameter which primarily affect the flow pattern in a column reactor.

Results with Predicted α - Distribution

In Fig.3, the results of the predictions are depicted where α-distribution was calculated from Eq.(14) directly. The inlet boundary condition was a step function, $\alpha=\alpha_o$ for $r/R < 0.5$ and $\alpha=0$ otherwise. The resulting recirculation pattern shown in Fig.3a is quite different than that in Fig.2a. The center of the recirculation zone moved towards the mid-hight of the reactor and the total circulated liquid volume, $Q_{cir}=0.12$ m^3/s, decreased. The corresponding α-distribution is shown in Fig.3b. The overall magnitude of α is lower in this case compared to that of Fig.2, and it does not vary much in the axial direction (see also Fig.3c). On the other hand, the centerline-gas velocity first increases and then decreases with the axial distance (Fig.3c) remaning fairly flat near the mid-hight of the column. Fig.3b also shows that narrow bubble street prescribed at the inlet is dispersed radially inward and outward as a result of convective gas velocities in this direction. A contour plot of α-distribution shown in Fig.3d indicates that first, the bubbles are convected towards the center of the tube near inlet then outwards towards the wall near the free surface, where the radial gas velocity (=liquid velocity) is inward and outward, respectively. This is in conformity with the usual experimental observations (e.g. Freedman and Davidson, 1969). In this case there is a much closer agreement between the measured and predicted velocity profile at

x/L=0.5 as shown in Fig.3e. The location of the measurements is reported (Rietema and Ottengraf, 1970) to be near the mid-hight of the column. The magnitude of the predicted u_ℓ values decreases because the overall α values are lower and hence less drag force is impacted on the liquid by the gas flow.

The value of the cut-off point (r/R=0.5) for the α-step function at x=0 was chosen arbitrarily. This brings the question of what exactly this value should be? Strictly speaking, this should be the location of the last row of injection holes on the distributor plate, but this information was not available from the experiments considered here. A further increase of this parameter to $r_s/R=0.66$ resulted in much closer agreement between the measured and predicted liquid velocities, but the center of the recirculation zone moved further down towards the inlet when the air flow was distributed over the whole cross-section of the inlet area, the resulting circulation was negligibly small.

CONCLUSIONS

Numerical calculations of the liquid circulation inside on isothermal column reactor has been performed in two steps: (a) with a prescribed α-profile (shape); (b) with α-distribution calculated from the transport equation for it.

The results indicate that the actual shape of the α-profile is not that critical with respect to the circulation patterns and the liquid velocity. The overall magnitude of the void fraction as well as the bubble-street diameter seems to be more important.

The predictions including the direct solution for α-distribution leads to a more realistic picture as compared to experimental observations. The boundary condition for α at the inlet (i.e. the distributor plate) seems to play a dominant role in determining the overall circulation pattern. At this point

numerical investigations need more input from experimental investigations.

The present mathematical model based on the continuum approach and the slip velocity relation seems to predict the overall characteristics of the circulation in the bubbly flow regime.

The full numerical solution of both the liquid and gas phases needs to be further investigation as well as the flow regimes other than the bubbly flow regime.

ACKNOWLEDGMENT

This work was sponsored by the U.S.DOE Pittsburgh Energy Technology Center under the contract No. DE-FG-87PC79935. The calculations were performed on the State of West Virginia Computer Network.

The authors would like to thank Dr. Nigel Clark and Dr. John Kuhlman for their valuable discussions.

REFERENCES

-Anderson, T.B. and R.G. Jackson (1967), "A Fluid Mechanical Description of Fluidized Beds," Industrial and Engineering Chemistry Fundamentals, Vol.6, No.4, pp.527-539.

-Clark, N, J. Kulhman and I. Celik (1990), "Circulation in Gas-Slurry Column Reactors," Final Report, Mechanical and Aerospace Engineering Dept., West Virginia University, Morgantown, WV (USA). U.S. DOE Pittsburgh Energy Technology Center Contract No: DE-FG-87PC79935.

-Celik, I. , "Computational Fluid Dynamics Assessment", Quarterly Technical Rept., Mech. & Aero. Engr. Dept., Oct. 1985-Jan. 1986, West Virginia Univ., 1986.

-Clift, R., J.R. Grace and M.E. Weber, Bubbles, Drops, and Particles, Academic Press, 1978.

-Drew, D.A. (1983) "Continuum Modeling of Two-phase Flows," in Theory of Dipersed Multiphase Flow, Editor: R.E.Meyer, Academic Press, New York, pp.173-190.

-Durst, F., and Loy, T. (1984) "TEACH: Ein Berechnungsverfahren fuer zweidimensionale laminare and turbulente Stroemungen," Report. Institut fuer Hyromechanik, Universtaet Karlsruhe, Karlsruhe, F.R.Germany.

-Freedman, W. and J.F. Davidson, "Holdup and Liquid Circulation in Bubble Columns", Trans. I. Chem. E., Vol.47, 1969, pp. T251-T262.

-Gosman, A.D. and F.J.K. Ideriah (1976), "Teach-2E: A General Computer Program for Two-Dimensional, Turbulent Recirculating Flows," Report without number, Dept. of Mech. Engrg, Imperial College. London.

-Hewitt, G.F., "Liquid-gas System: Void Fraction", in Handbook of Multiphase Systems, Hetsroni, G. ed., Hemisphere Publishing Corporation, McGraw-Hill Publishing Company, 1982.

-Hill, J.H., "Radial Non-Uniformity of Velocity and Voidage in a Bubble Column", Trans. I. Chem.E., Vol.52, 1974, pp.1-9.

-Hinze, J.O., "Turbulent Fluid and Particle Interaction", Progress in Heat and Mass Transfer, 6, Oxford, 1972, pp.433-452.

-Hirt, C.W., "Numerical Fluid Dynamics", A short course, Flowscience Inc., Los Alamos, New Mexico, 1982.

-Homsy, G.M. (1983), "A survey of Some Results in the Mathematical Theory of Fluidzation," in Theory of Dispersed Multiphase Flow, Editor: R.E. Meyer, Academic Press, New York, pp.57-70.

-Lamont, A.G.W., "Air Agitation and Pachuca Tanks", Can. Jour. Chem. Eng., August 1958, pp-153-160.

-Patankar, S.V., (1980) Numerical Heat Transfer and Fluid Flow, Hemisphere Publ. Corp., New York.

-Rietema, K., "Science and Technology of Dispersed Two Phase Systems", Chem. Eng. Sci, Vol.37, 1982, pp.1125-1150.

-Rietema, K. and Ottengraf, S.P.P., (1970) "Laminar Liquid Circulation and Bubble Street Formation in a Gas-Liquid System." Trans. Inst. Chem. Engrs., Vol.48, pp.T54-T62.

-Steinemann, J. Buchholz, R., "application of an Electrical Conductuvuty Microprobe for the Characterization of Bubble Behavior in Gas-liquid Bubble Flow," Particle Characterization, Vol.1, 1984, pp.102-107.

-Stewart, H.B. and B. Wendroff (1984), "Two-Phase Flow: Models and Methods", J.Comput. Phys. 56, pp.363-409.

-Syamlal, M. and O'Brien, T.J., "Simulation of Granular Layer Inversion in Liquid Fluidized Beds," Int. J. Multiphase Flow, 14, No.4, 1988, pp.473-481.

-Wallis, G.B., in Rottenburg, P.A.(Ed.), "Interaction Between Fluids and Particles", 1962, p.9, (London, The Institution of Chemical Engineers).

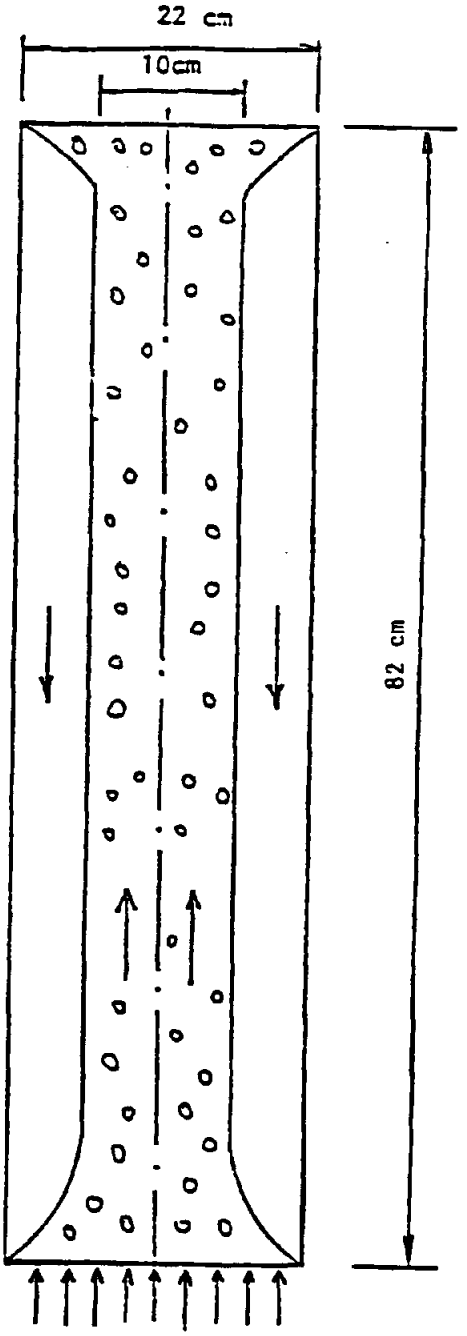

Fig.1 Geometry of the bubble column
(Experiments by Rietema and Ottengraf, 1970)

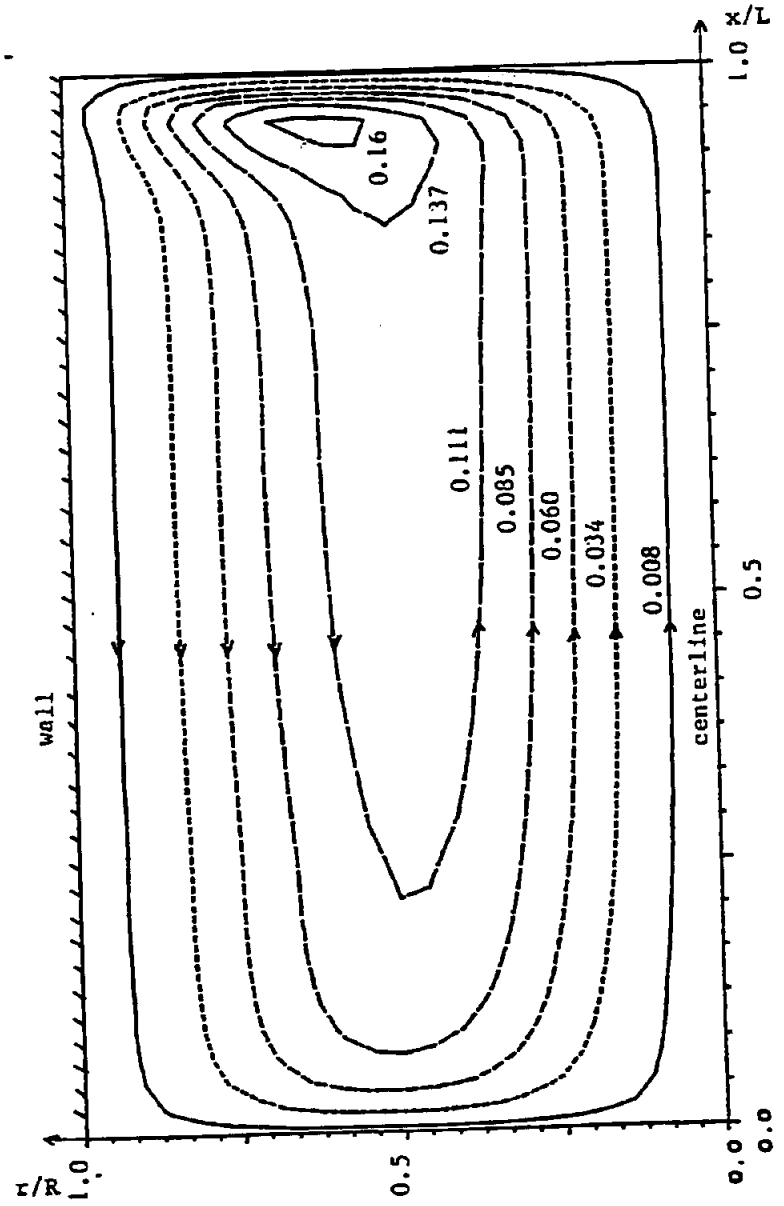

Fig.2 (a) Calculated circulation patterns

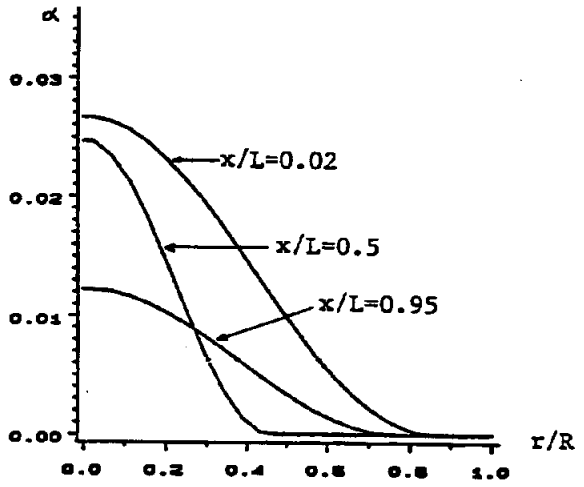

Fig.2 (b) Calculated α - distribution

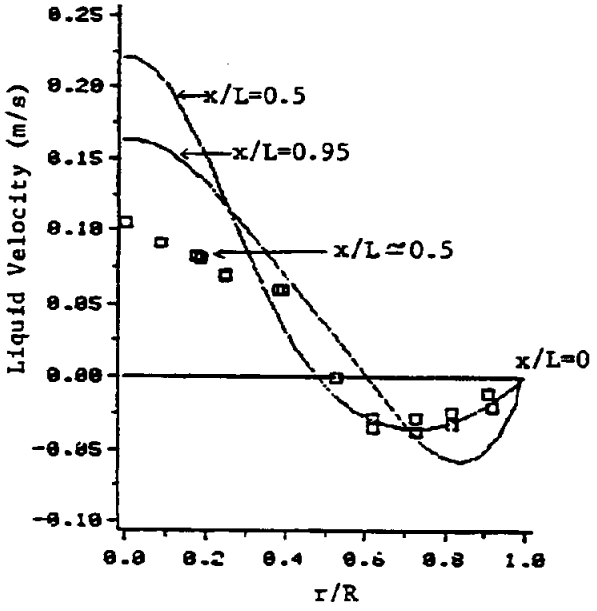

Fig.2 (c) Liquid velocity profiles

Fig.2 Predictions using a cosine profile for α (Eq.12)
□- Experiment (Rietema and Ottengraf, 1970)

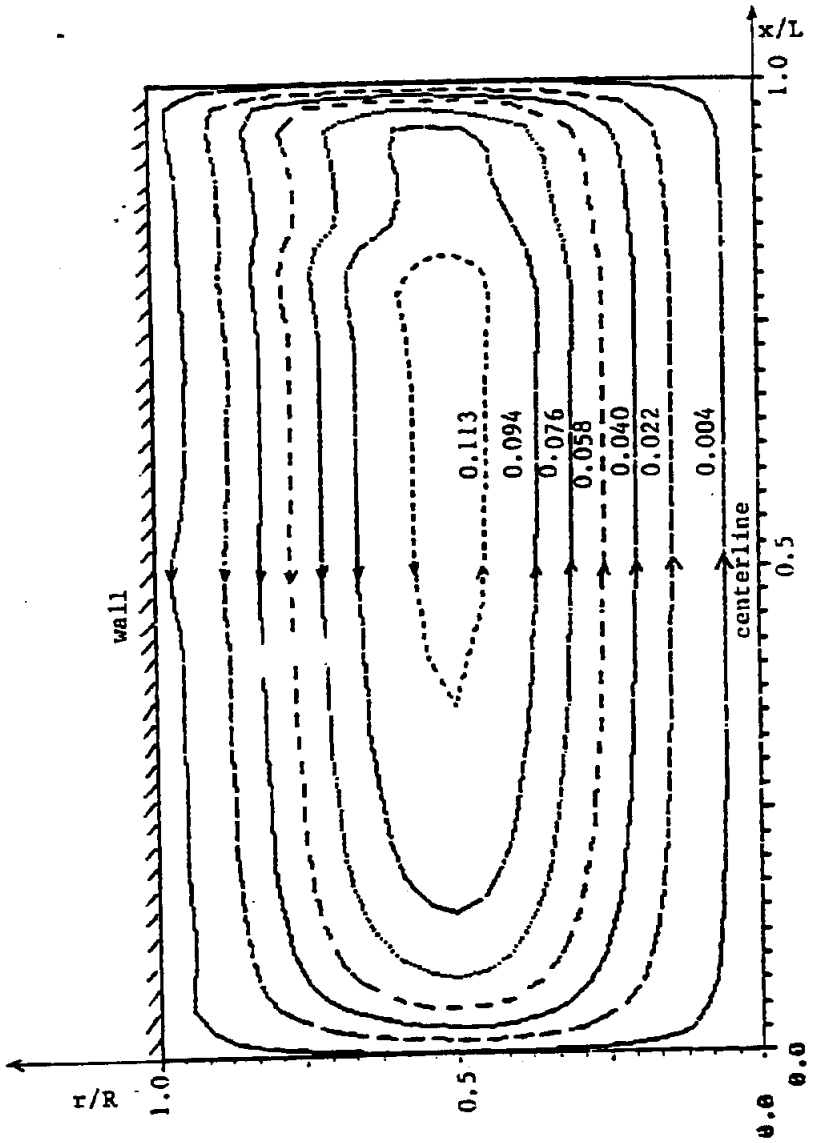

Fig.3 (a) Calculated circulation pattern ($r_s/R=0.45$)

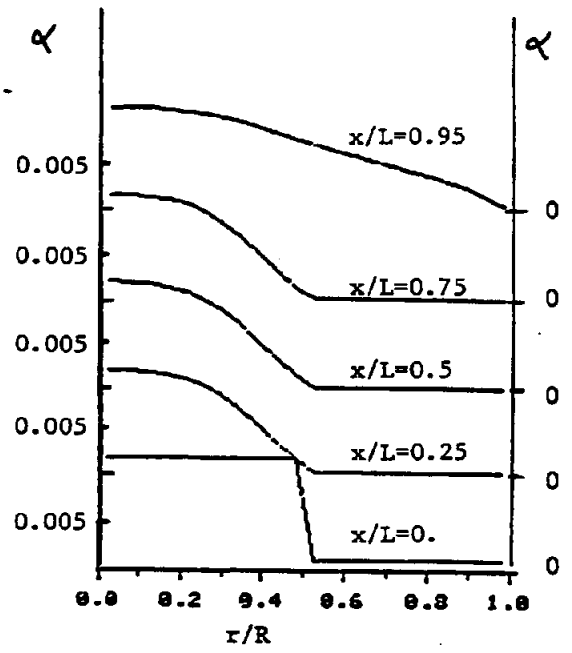

Fig.3 (b) α - distribution

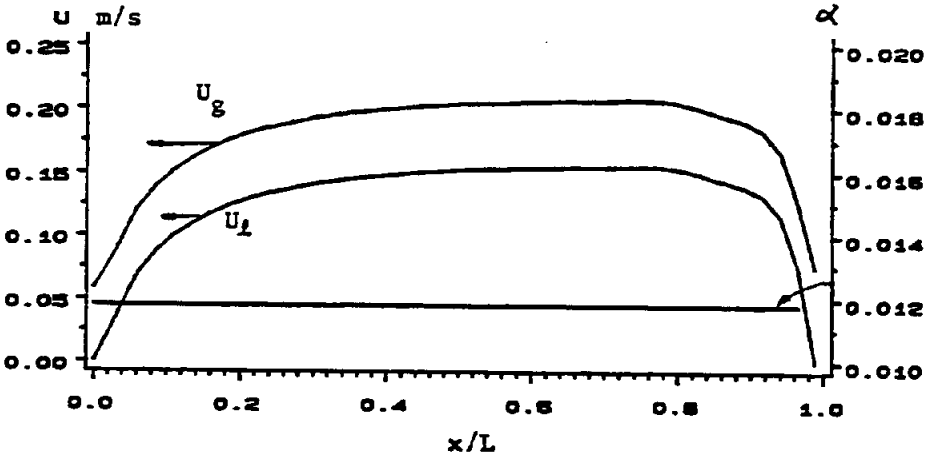

Fig.3 (c) Liquid velocity, gas velocity and α distribution along the centerline of the column

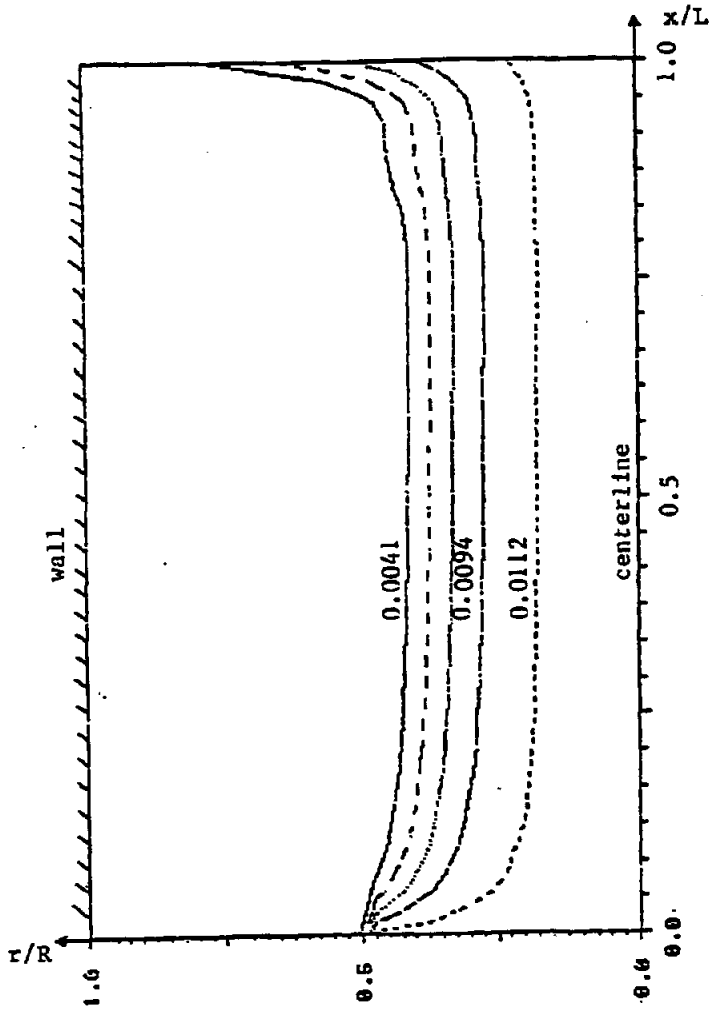

Fig.3 (d) α contours

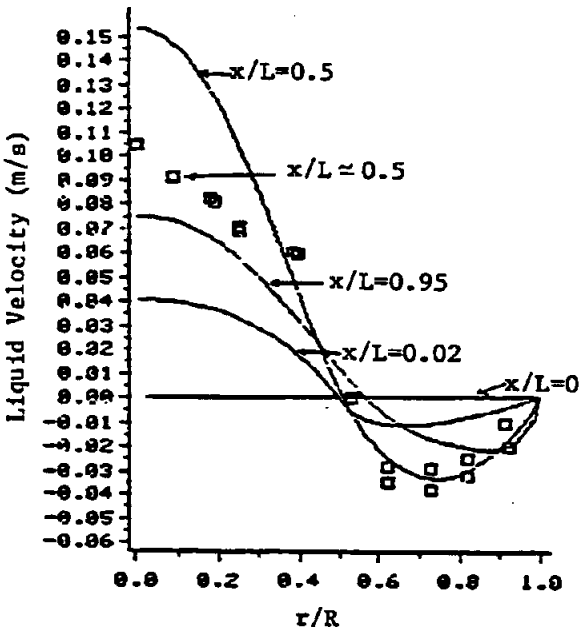

□ - Experiment (rietema and Ottengraf, 1970)

Fig.3 (e) Liquid velocity profiles

Fig.3 Prodictions with α-distribution calculated from the transport equation